

Research Article

An Optimization Theoretic Framework for Video Transmission with Minimal Total Distortion over Wireless Networks

Pejman Goudarzi, Mohammad Hesam Tadayon, and Mahmoud Mousavinejad

Multimedia Group, IT Faculty, Iran Telecom Research Center (ITRC), P.O. Box 14155-3961, Tehran 14399 55471, Iran

Correspondence should be addressed to Pejman Goudarzi, pgoudarzi@itrc.ac.ir

Received 17 February 2008; Revised 4 October 2008; Accepted 10 January 2009

Recommended by Kameswara Namuduri

Optimization theoretic-based rate allocation strategies can be used for the aim of allocating some optimal rates to the competing users in wireless ad hoc networks. By considering different objective functions (such as congestion level, total packet loss, etc.), the researchers propose some optimization framework by which the problem can be solved. Due to the rapid increase in the development of different video applications in such environments and the existence of difficulties in satisfying the prespecified QoS limits, increasing the perceived video quality can be considered as an important and challenging issue. The quality of the received video stream is inversely proportional to the amount of distortion which is being imposed on the video stream by the network packet loss and the video encoder. The main contribution of the current paper is to introduce an optimization theoretic framework in which by optimal rate allocation to some competing video sources, the aggregate distortion associated with all of the sources can be minimized. The numerical results verify the claims.

Copyright © 2009 Pejman Goudarzi et al. This is an open access article distributed under the Creative Commons Attribution License, which permits unrestricted use, distribution, and reproduction in any medium, provided the original work is properly cited.

1. Introduction

Convex optimization theory is an important tool for many rate allocation algorithms in wireline or wireless networks. Wireless ad hoc networks are computer networks in which the communication links are wireless. The network is ad hoc because each node is willing to forward data for other nodes, and so the determination of which nodes forward data is made dynamically based on the network connectivity. This is in contrast to wired network technologies in which some designated nodes, usually with custom hardware (variously known as routers, switches, hubs, and firewalls), perform the task of switching and forwarding the data. Ad hoc networks are also in contrast to managed wireless networks, in which a special node known as an access point manages communication among other nodes. Ad hoc networks can form a network without the aid of any pre-established infrastructure [1].

The requirements of a specific set of QoS parameters (delay, jitter, packet loss, etc.) must be guaranteed for each real-time application. However, for most real-time applications of wireless ad hoc networks, intrinsic

time-varying topological changes provide challenging issues in guaranteeing these stringent QoS requirements.

Due to dynamic nature of these networks, traditional routing protocols are useless. So, special proactive/reactive multihop routing protocols such as DSDV/AODV are developed. Some of these routing protocols introduce more than one feasible path for a source-destination pair. These categories of routing algorithms are called multipath routing algorithms [2]. Multipath routing schemes can reduce interference, improve connectivity, and allow distant nodes to communicate efficiently [2]. In multipath routing, multiple multihop routes or paths are used to send data to a given destination. This allows a higher spatial diversity gain and throughput between source and destination nodes. On the other hand, it is obvious that inherent load balancing feature of the multipath routing algorithms has the capability of reducing the congestion as well as increasing the throughput of the user traffic in multihop wireless ad hoc networks. Moreover, using multiple paths between any source-destination pair can improve the important reliability and availability features of the routing strategy.

Multipath routing can provide both diversity and multiplexing gain between source and destination. However, multihop and multipath routing can also increase the total packet loss between the source and destination, especially if there is congestion in the paths or if the bit error rate of the paths is high due to the bad wireless link conditions (existence of high noise or interference levels). Therefore, supporting multimedia data with stringent maximum loss requirement over multihop ad hoc networks with multipath routing can be considered as an important and challenging research area.

Sending multimedia traffic over wireless ad hoc networks is a challenging issue, and many active research areas exist that all try to propose a solution to the problem from different points of view.

Some researchers such as those in [3, 4] try to use adaptive link layer techniques for throughput optimization. The authors in [4] propose a mathematical framework in which they vary adaptively the constellation size of an MQAM modulator in order to maximize the single user throughput.

In [5, 6] a congestion-minimized stream routing approach is adopted. In [6] the authors analyze the benefits of an optimal multipath routing strategy which seeks to minimize the congestion, on the video streaming, in a bandwidth limited ad hoc wireless network. They also predict the performance in terms of rate and distortion, using a model which captures the impact of quantization and packet loss on the overall video quality.

Some researchers such as Agarwal [7], Adlakha [8], and Zhu [9] follow some congestion-aware and delay-constrained rate allocation strategies. Agarwal and Goldsmith [7] introduce a mathematical constrained convex optimization framework by which they can jointly perform both rate allocation and routing in a delay-constrained wireless ad hoc environment. Adlakha et al. extend the conventional-layered resource allocation approaches by introducing a novel cross-layer optimization strategy in order to more efficiently perform the resource allocation across the protocol stack and among multiple users. They showed that their proposed method can support simultaneous multiple delay-critical application sessions such as multiuser video streaming [8].

For multipath video streaming over ad hoc wireless networks, received video quality is influenced by both the encoder performance and the delayed packet arrivals due to limited bandwidth. Hence, Zhu et al. propose a rate allocation scheme to optimize the expected received video quality based on simple models of encoder rate-distortion performance and network rate-congestion trade-offs [9]. As the quality of wireless link varies, video transmission rate needs to be adapted accordingly.

In [6], Setton et al. analyzed the benefits of optimal multipath routing on video streaming in a bandwidth-limited ad hoc network. They show that in such environments the optimal routing solutions which seek to minimize the congestion are attractive as they make use of the resources efficiently. For low-latency video streaming, they propose to limit the number of routes to overcome the limitations of

such solutions. To predict the performance in terms of rate and distortion, they develop a model which captures the impact of quantization and packet loss on the overall video quality.

In [10], measurements of packet transmission delays at the MAC layer are used to select the optimal bit rate for video, subsequently enforced by a transcoder. The benefit of cross-layer signaling in rate allocation has also been demonstrated in [11], where adaptive rate control at the MAC layer is applied in conjunction with adaptive rate control during live video encoding. The authors in [12] propose a media-aware multiuser rate allocation algorithm in multihop wireless mesh networks that can adjust the video rate adaptively based on both video content and network congestion and show the benefits of their work with respect to the well-known TCP friendly rate control (TFRC) [13].

In the current work, a similar approach such as [7] is being adopted by which a constrained optimization framework is introduced for optimal rate allocation to the real-time video applications. In [6], the authors do a similar optimization but they take the average congestion of the overall network as the QoS criterion and minimize it to find the optimal solution for rate allocation on the available paths using simulations. In [14], the authors propose a distributed rate allocation algorithm which minimizes the total distortion of all video streams. Based on the subgradient method, their proposed scheme only requires link price updates at each relay node based on local observations and rate adaptations at each source node derived from rate-distortion (RD) models of the video. They show by simulation that their proposed scheme can achieve the same optimal rate allocation as that obtained from exhaustive search.

The presented work in this paper differs from that of [14] in that, in our work, we have assumed that each video source may use multipath routing for partitioning and transmission of the total video traffic. On the other hand, we have included the effect of the packet loss in the perceived video distortion. Our work differs from [6, 7] in that we have used the total distortion as an objective Quality of Experience (QoE) measure in place of the QoS criterion used in [6, 7]. In order to compute the total distortion, we have assumed that multiple video sources use the same wireless ad hoc medium for transmission, and their associated distortions are additive [6]. On the other hand, the presented work differs from [7] in considering more than one (and possibly interfering) multipath-routed video sources which compete for the available bandwidth in a bandwidth-limited wireless ad hoc network.

The paper's objective is to develop an optimal rate allocation framework bases on which the overall distortion of all the video sources is minimized. We also have used a penalty function approach for finding an iterative solution algorithm for the proposed constrained optimization problem such as those introduced in [15, 16].

The rest of the paper is organized as follows. In Section 2 the relationship between the allocated rate and the resulting distortion is introduced. In Section 3 the proposed optimization framework has been developed in detail. Section 4 is

devoted to the numerical analysis, and finally in Section 5 some concluding remarks are presented.

2. Video Distortion Model

For smooth playback of a live video, transmitted packets must meet maximum allowed delay constraint. Therefore, the packets with a greater delay are useless so that they are supposed as packet loss. On the other hand, the total distortion of decoded video is the superposition of the distortion caused by video encoder (\mathcal{D}_{enc}) and the distortion caused by packet loss or late arrivals during the transmission ($\mathcal{D}_{\text{trans}}$) [6].

According to [17], considering Mean Squared Error (MSE) criterion and assuming that \mathcal{D}_{enc} and $\mathcal{D}_{\text{trans}}$ are uncorrelated, the overall distortion can be written as follows:

$$\mathcal{D}_{\text{dec}} = \mathcal{D}_{\text{enc}} + \mathcal{D}_{\text{trans}}. \quad (1)$$

The empirical Rate-Distortion (R-D) model in [17] is used to represent \mathcal{D}_{enc} :

$$\mathcal{D}_{\text{enc}} = \mathcal{D}_0 + \frac{\theta}{\mathcal{R} + \mathcal{R}_0}, \quad (2)$$

where \mathcal{R} is the rate of encoded video, and the parameters \mathcal{D}_0 , $\theta > 0$, and \mathcal{R}_0 are calculated empirically from R-D curves. Again, based on [17], we assume a linear relationship between the total packet error rate (PER) and $\mathcal{D}_{\text{trans}}$:

$$\mathcal{D}_{\text{trans}} = \xi \cdot p_T, \quad (3)$$

where p_T is the PER, and the scaling factor $\xi > 0$ depends on the encoding structure. Assuming that the video encoder uses the maximum allocated channel capacity, the rate of encoded video can be computed as follows [6]:

$$\mathcal{R} = \sum_{j=1}^n x_j, \quad (4)$$

where n is the number of paths in a multipath-routed source-destination pair, and x_j is the rate allocated to the j 'th path. The above assumption is achievable by using adaptive source rate control algorithms such as those mentioned in [18–20].

3. Proposed Optimization Framework

Consider the multihop wireless ad hoc network depicted in Figure 1. Assume that there exist \mathcal{N} video sources, and the existing multipath routing protocol (e.g., DSDV) introduces n_k disjoint multihop paths between each source-destination pair (S_k, D_k) periodically ($1 \leq k \leq \mathcal{N}$). Each path is associated with a traffic flow, and these multiplexed flows are aggregated in the destination node to produce the initial source-generated traffic stream. The number n_k is selected based on the assumption of availability of the current paths throughput information for the video source node S_k and the sufficiency of the aggregate-estimated throughput for the traffic's minimum bandwidth requirements.

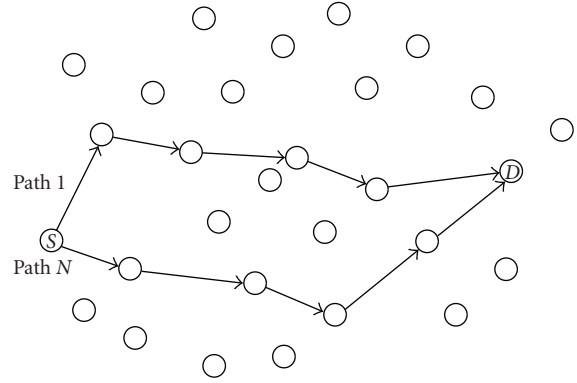


FIGURE 1: A typical multihop wireless ad hoc network.

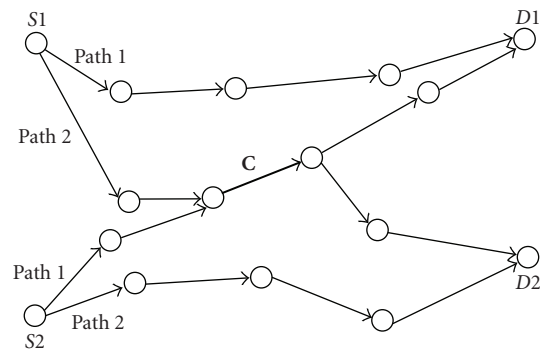


FIGURE 2: Two competing multipath-routed video sources.

Each path j related to the source k contains \mathcal{M}_{jk} wireless links from source to destination for $1 \leq k \leq \mathcal{N}$ and $1 \leq j \leq n_k$. We assume that the total capacity of the wireless link ℓ between the nodes y and z is denoted by \mathcal{C}_ℓ and is derived as follows [6]:

$$\mathcal{C}_\ell = \frac{W}{2} \log(1 + \gamma \text{SNR}_\ell), \quad (5)$$

where SNR_ℓ is the Signal to Noise Ratio between the nodes y and z and can be written as follows:

$$\text{SNR}_\ell \triangleq \frac{d_{yz}^{-\alpha}}{WN}. \quad (6)$$

In the above calculations it is assumed that by a properly designed MAC protocol, there exist no collisions so that the inter node interference (INI) can be neglected. d_{yz} is the distance between node y and node z , α denotes the path loss exponent, N represents the power spectral density of the noise, W is the system bandwidth, and γ is the coding gain. It is also assumed that the transmission power is equal at all nodes. In the following, we will assume that the nodes are static with $\alpha = 2$. While this is a simplified model for the wireless ad hoc network, the analysis we present can easily be extended to the more sophisticated link capacity calculations.

We assume a simple strong line of sight (LOS) with BPSK signaling for node's wireless transmissions and also neglect the interfering effect of wireless transmissions between

different paths [1]. We have used the Independent Basic Service Set (IBSS) setup (DCF mode) for implementing the MAC layer of the 802.11 WLAN standard which enforces the WLAN network in the ad hoc mode. It is assumed that BPSK DSSS is used in the physical layer. As the Bit Error Rate (BER) performance of the BPSK spread spectrum system in an AWGN environment is identical to that of conventional coherent BPSK system [21], it is sufficient to calculate the latter performance for evaluating the BER of the proposed system.

We also assume that the transmitted data is fragmented in equal length packets of length L bits enabled with FEC error correction capability up to M bits, and this leads to the coding gain γ .

In the current paper, our objective is to minimize the total distortion associated with multiple video sources. Thus, a mathematical formulation must be presented to express the distortion of each video source in terms of its allocated rate. According to (3), this distortion is a function of the PER associated with each video source. In the following paragraphs, the packet error rate computation method is presented.

The bit error rate (BER) of the link i in the j 'th path of the k 'th video source can be represented for a simple strong LOS propagation model with BPSK signaling as follows [1]:

$$b_{ijk} = Q\left(\frac{\eta_{ijk}}{\sqrt{r_{ijk}}}\right) \quad \begin{array}{l} 1 \leq i \leq \mathcal{M}_{jk}, \\ 1 \leq j \leq n_k, \\ 1 \leq k \leq \mathcal{N}, \end{array} \quad (7)$$

where

$$\eta_{ijk} = h_{ijk} \cdot \sqrt{\mathcal{T}_{ijk}} \quad \forall k, j, i \in \mathcal{R}_{jk}, \quad (8)$$

$$Q(y) \triangleq \frac{1}{\sqrt{2\pi}} \int_y^\infty e^{-x^2/2} dx,$$

where h_{ijk} is a physical constant, \mathcal{R}_{jk} is the (nonempty) set of wireless links associated with the j 'th flow of the k 'th video source, and \mathcal{T}_{ijk} and r_{ijk} are the transmitted power and the total transmission rate associated with the i 'th link in the j 'th flow of the k 'th source, respectively. As it is said before, we assume that \mathcal{T}_{ijk} is fixed during transmission and therefore does not depend on the transmission data rate r_{ijk} .

Assume that \mathcal{R}_{jk} can be partitioned in two disjoint subsets. One subset is associated with those wireless links that are common between more than one video sources which we denote by \mathcal{R}_{jk}^c (it is assumed that this subset is not empty for at least one j), and the other set contains noncommon wireless links which we denote by \mathcal{R}_{jk}^{nc} . So, we can write

$$\mathcal{R}_{jk} = \mathcal{R}_{jk}^c \cup \mathcal{R}_{jk}^{nc} \quad \forall j, k. \quad (9)$$

We represent the set cardinality operator by $|\cdot|$, so we have $|\mathcal{R}_{jk}| = \mathcal{M}_{jk}$. We also assume that $|\mathcal{R}_{jk}^{nc}| = \mathcal{O}_{jk}$, and thus we have $|\mathcal{R}_{jk}^c| = \mathcal{M}_{jk} - \mathcal{O}_{jk}$.

The r_{ijk} consists of two components: one is the traffic rate allocated to the j 'th flow of the k 'th source which is denoted by x_{jk} , and the other part is associated with the time-varying i 'th link's cross (background) traffic a_{ijk} . Thus we have

$$r_{ijk} = x_{jk} + a_{ijk} \quad \forall k, j, i \in \mathcal{R}_{jk}. \quad (10)$$

So, the available capacity (throughput) is denoted by e_{ijk} and is equal to $e_{ijk} = \mathcal{C}_{ijk} - a_{ijk}$, where \mathcal{C}_{ijk} is the capacity of the link i in the j 'th path of the k 'th video source.

In some cases (as is depicted in Figure 2), two or more multipath video sources may compete for a *common* wireless link (in Figure 2 this link is shown by bold line). Therefore, the available capacity of the common link must be shared between the competing flows in an optimal manner.

Assume that for each common link $i \in \mathcal{R}_{jk}^c$ there exists an associated set \mathcal{S}_{jk}^i which represents the set of all ordered pairs (*path, source*) that use the common link i in the path j of the source k (e.g., in Figure 2, the path 1 of source 2 shares the common link C with the path 2 of source 1). So the ingress and egress nodes associated with this common link are common between more than one flow.

For common links we assume that background traffic is composed only of those flows which are in \mathcal{S}_{jk}^i , that is, we can write

$$a_{ijk} = \sum_{(u,v) \in \mathcal{S}_{jk}^i} x_{uv} \quad \forall k, j, i \in \mathcal{R}_{jk}^c. \quad (11)$$

With the assumption of independent links' bit error rate, the total bit error rate along the j 'th path of the k 'th source can be calculated as follows:

$$\mathcal{B}_{jk} = 1 - \prod_{i=1}^{\mathcal{M}_{jk}} (1 - b_{ijk}) \quad \forall j, k. \quad (12)$$

The total PER of the j 'th path of the k 'th video source is composed of the congestion-related and noncongestion-related (wireless link) losses which we denote by $p_{jk}^{\mathcal{Q}}$ and $p_{jk}^{\mathcal{R}}$, respectively.

If the FEC-induced error correction capability of a packet with length L bits is M bits ($M > 1$) and with the assumption of independent bit errors (lack of burst errors), the wireless link-related PER along the j 'th path (flow) of the k 'th source can be calculated as follows:

$$p_{jk}^{\mathcal{R}} = 1 - \sum_{m=0}^M \binom{L}{m} \mathcal{B}_{jk}^m (1 - \mathcal{B}_{jk})^{L-m} \quad \forall j, k. \quad (13)$$

Now we are in a position that must compute the congestion-related part of the PER.

First, assume that the end-to-end queuing delay of the j 'th path of the k 'th source can be represented with a random variable with the probability density function (*pdf*) $\beta_{jk}(t)$.

By adopting the same approach as in [7], it can be assumed that congestion-related packet loss occurs when the end-to-end queuing delay of the j 'th path of the k 'th source exceeds a predetermined threshold Δ_{jk} . In mathematical terms the mentioned fact can be represented as follows:

$$p_{jk}^{\mathcal{Q}} = \int_{\Delta_{jk}}^\infty \beta_{jk}(t) dt \quad \forall j, k. \quad (14)$$

In the sequel, the distribution $\beta_{jk}(t)$ has been calculated based on some specific assumptions.

As in [7] simple M/M/1 queuing model and FIFO service discipline are adopted for the nodes. With the

assumption of M/M/1 queueing model, the service time of each queue is an exponentially distributed random variable [22]. We also assume that this service times are independent. On the other hand, the end-to-end delay of each path j belonging to the video source k is equal to the sum of these independent random variables. Ignoring the source and destination nodes (hops), the total number of nodes in \mathcal{R}_{jk} and the number of noncommon nodes in \mathcal{R}_{jk}^{nc} and common nodes in \mathcal{R}_{jk}^c would be $\mathcal{M}_{jk} - 1$, $\mathcal{O}_{jk} - 2$, and $\mathcal{M}_{jk} - \mathcal{O}_{jk} + 1$, respectively, for each j, k .

3.1. Definition. If traffic flows from node a to node b , the nodes a and b are called the *ingress* and *egress* nodes for the link ab , respectively.

Based on [23], for the nodes in \mathcal{R}_{jk} , the delay distribution (*pdf*) can be represented by *exponential* distribution as follows:

$$f_{ijk}(t) = \frac{e^{-t/\alpha_{ijk}}}{\alpha_{ijk}} \quad \forall k, j, i \in \mathcal{R}_{jk}, \quad (15)$$

where we can write for noncommon nodes associated with \mathcal{R}_{jk}^{nc} [8]:

$$\alpha_{ijk} = \frac{1}{e_{ijk} - x_{jk}} \quad \forall j, k, i \in \mathcal{R}_{jk}^{nc}. \quad (16)$$

Based on the value of e_{ijk} and for ingress/egress nodes associated with common links in \mathcal{R}_{jk}^c , we can write [8]

$$\alpha_{ijk} = \left(\mathcal{O}_{ijk} - \sum_{(u,v) \in \mathcal{S}_{jk}^c} x_{uv} - x_{jk} \right)^{-1} \quad \forall k, j, i \in \mathcal{R}_{jk}^c. \quad (17)$$

Thus the probabilistic distribution function of the end-to-end delay ($\beta_{jk}(t)$) is the convolution of all these *pdf*'s [22]. On the other hand, we can write

$$\beta_{jk}(t) = \overbrace{f_{1jk}(t) * \dots * f_{njk}(t)}^{\mathcal{M}_{jk}-1} \quad \forall j, k, \quad (18)$$

where $n = \mathcal{M}_{jk} - 1$ is the number of nodes in \mathcal{R}_{jk} , $*$ is the *convolution* operator, and $f_{1jk} \dots f_{njk}$ are the *pdf*'s associated with all of the nodes which reside in \mathcal{R}_{jk} .

The total PER related to the j 'th flow of the k 'th source can be simply shown to be equal to

$$p_{jk} = 1 - (1 - p_{jk}^{\mathcal{R}})(1 - p_{jk}^{\mathcal{Q}}) \quad \forall j, k. \quad (19)$$

The total PER of the source-destination pair k with the assumption of independent path packet losses can be written as follows:

$$p_T^k = 1 - \prod_{j=1}^{n_k} (1 - p_{jk}) \quad \forall k. \quad (20)$$

We also define the total allocated rate to the source k to be \mathcal{R}_k , and we have

$$\mathcal{R}_k = \sum_{j=1}^{n_k} x_{jk} \quad \forall k. \quad (21)$$

As described in (1)–(4), we can formulate the distortion of each video source k (\mathcal{D}_k) as follows [6]:

$$\mathcal{D}_k = \mathcal{D}_{k0} + \frac{\theta_k}{\mathcal{R}_k + \mathcal{R}_{k0}} + \xi_k \cdot p_T^k \quad \forall k. \quad (22)$$

Based on the above facts, the formulation of the proposed total distortion minimization problem can be done as follows:

$$\min \mathcal{D}_T \triangleq \sum_{k=1}^{\mathcal{N}} \mathcal{D}_k \quad (23)$$

subject to

$$\sum_{j=1}^{n_k} x_{jk} \geq x_{k,\min} \quad \forall k \quad (24)$$

$$0 \leq x_{jk} \leq \min_i(e_{ijk}) \quad \forall j, k, i \in \mathcal{R}_{jk}, \quad (25)$$

in which $x_{k,\min}$ is the minimum required bandwidth for the k 'th video source.

We must now remind our previous assumption that the parameter n_k is assumed to be large enough such that the constraint (24) is met for all k .

Suppose that the optimal solution vector of the system (23)–(25) is defined as follows:

$$\chi^* \triangleq (x_{11}^*, x_{21}^* \dots x_{n_1}^* \dots x_{1\mathcal{N}}^* \dots x_{n_{\mathcal{N}}}^*). \quad (26)$$

Since the constraint set is convex, in order to make the constrained optimization problem (23)–(25) has a unique and optimal solution vector χ^* , it is necessary and sufficient that the following Lagrangian equation to have positive second derivatives with respect to all of the x_{jk} variables [16]:

$$\begin{aligned} \Psi(\chi) \triangleq & \mathcal{D}_T - \sum_{k=1}^{\mathcal{N}} \lambda_k \left(\sum_{j=1}^{n_k} x_{jk} - x_{k,\min} \right) \\ & - \sum_{k=1}^{\mathcal{N}} \sum_{j=1}^{n_k} \lambda_{jk} \left(\min_i(e_{ijk}) - x_{jk} \right), \end{aligned} \quad (27)$$

where λ_{jk} and λ_k are the Lagrange multipliers.

Theorem 1. Consider a typical multihop wireless ad hoc network. Assume that the following assumption holds:

$$0 \leq \mathcal{B}_{jk} < \frac{1}{L} \quad \forall j, k. \quad (28)$$

Then, there exists some M such that the following holds:

$$\frac{\partial^2 p_{jk}^{\mathcal{R}}}{\partial r_{mjk} \partial r_{njk}} > 0 \quad \forall k, j, m, n \in \mathcal{R}_{jk}. \quad (29)$$

Proof. From (13) we have

$$\frac{\partial p_{jk}^{\mathcal{R}}}{\partial r_{mjk}} = -\frac{\partial \mathcal{B}_{jk}}{\partial r_{mjk}} \varphi_{jk} \quad \forall k, j, m \in \mathcal{R}_{jk}, \quad (30)$$

where

$$\varphi_{jk} \triangleq \sum_{m=1}^M \binom{L}{m} (m - L \cdot \mathcal{B}_{jk}) \mathcal{B}_{jk}^{m-1} (1 - \mathcal{B}_{jk})^{L-m-1} - L \cdot (1 - \mathcal{B}_{jk})^{L-1} \quad \forall i. \quad (31)$$

Similarly we can write

$$\frac{\partial^2 p_{jk}^{\mathcal{R}}}{\partial r_{mjk} \partial r_{njk}} = -\varphi_{jk} \frac{\partial^2 \mathcal{B}_{jk}}{\partial r_{mjk} \partial r_{njk}} - \psi_{jk} \frac{\partial \mathcal{B}_{jk}}{\partial r_{mjk}} \cdot \frac{\partial \mathcal{B}_{jk}}{\partial r_{njk}} \quad \forall k, j, m, n \in \mathcal{R}_{jk}, \quad (32)$$

where we have for each j, k the following:

$$\begin{aligned} \psi_{jk} &= \frac{\partial \varphi_{jk}}{\partial \mathcal{B}_{jk}} \triangleq L(L-1)(1 - \mathcal{B}_{jk})^{L-3} [(L-1)\mathcal{B}_{jk} - 1] \\ &+ \sum_{m=2}^M \binom{L}{m} \mathcal{B}_{jk}^{m-2} (1 - \mathcal{B}_{jk})^{L-m-2} \\ &\cdot [m(m-1) - 2m(L-1)\mathcal{B}_{jk} + L(L-1)\mathcal{B}_{jk}^2]. \end{aligned} \quad (33)$$

From (12) and the definition of b_{ijk} in (7), we can write for all $k, j, m \in \mathcal{R}_{jk}$ the following:

$$\frac{\partial \mathcal{B}_{jk}}{\partial r_{mjk}} = \left[\prod_{\substack{n=1 \\ n \neq m}}^{\mathcal{M}_{jk}} (1 - b_{njk}) \right] \frac{\eta_{mjk} \cdot e^{-\eta_{mjk}^2/r_{mjk}}}{2\sqrt{2\pi}} r_{mjk}^{-3/2}, \quad (34)$$

$$\begin{aligned} \frac{\partial^2 \mathcal{B}_{jk}}{\partial r_{mjk} \partial r_{njk}} &= - \left[\prod_{\substack{u=1 \\ u \neq m, n}}^{\mathcal{M}_{jk}} (1 - b_{ujk}) \right] \\ &\cdot \frac{\eta_{mjk} \cdot \eta_{njk} \cdot e^{-\eta_{mjk}^2/r_{mjk}} \cdot e^{-\eta_{njk}^2/r_{njk}}}{8\pi} \\ &\cdot r_{mjk}^{-3/2} r_{njk}^{-3/2} \quad \forall k, j, m, n \in \mathcal{R}_{jk}, m \neq n \end{aligned} \quad (35)$$

and also

$$\begin{aligned} \frac{\partial^2 \mathcal{B}_{jk}}{\partial r_{ijk}^2} &= \left[\prod_{\substack{m=1 \\ m \neq i}}^{\mathcal{M}_{jk}} (1 - b_{mjk}) \right] \frac{\eta_{ijk} \cdot r_{ijk}^{-7/2} \cdot e^{-\eta_{ijk}^2/r_{ijk}}}{2\sqrt{2\pi}} \\ &\cdot \left(\eta_{ijk}^2 - \frac{3}{2} r_{ijk} \right) \quad \forall k, j, i \in \mathcal{R}_{jk}. \end{aligned} \quad (36)$$

Based on (34)-(35) it can easily be shown that

$$\frac{\partial \mathcal{B}_{jk}}{\partial r_{ijk}} > 0 \quad \forall k, j, i \in \mathcal{R}_{jk}, \quad (37)$$

$$\frac{\partial^2 \mathcal{B}_{jk}}{\partial r_{mjk} \partial r_{njk}} < 0 \quad \forall k, j, m, n \in \mathcal{R}_{jk}, m \neq n. \quad (38)$$

We define

$$\Phi_{jk}^{mn}(\mathcal{B}_{jk}) \triangleq \frac{\partial^2 p_{jk}^{\mathcal{R}}}{\partial r_{mjk} \partial r_{njk}} \quad \forall k, j, m, n \in \mathcal{R}_{jk}, m \neq n. \quad (39)$$

Also we can write

$$\frac{\partial^2 p_{jk}^{\mathcal{R}}}{\partial r_{ijk}^2} = -\varphi_{jk} \frac{\partial^2 \mathcal{B}_{jk}}{\partial r_{ijk}^2} - \psi_{jk} \left(\frac{\partial \mathcal{B}_{jk}}{\partial r_{ijk}} \right)^2 \quad \forall k, j, i \in \mathcal{R}_{jk}. \quad (40)$$

We also introduce

$$\Phi_{jk}^i(\mathcal{B}_{jk}) \triangleq \frac{\partial^2 p_{jk}^{\mathcal{R}}}{\partial r_{ijk}^2} \quad \forall k, j, i \in \mathcal{R}_{jk}. \quad (41)$$

(a) Consider the case $m \neq n$.

Based on (32) and (34)-(35), we can simplify Φ_{jk}^{mn} to the following form:

$$\begin{aligned} \Phi_{jk}^{mn} &= -\frac{\partial^2 \mathcal{B}_{jk}}{\partial r_{mjk} \partial r_{njk}} \cdot (\varphi_{jk} - (1 - \mathcal{B}_{jk})\psi_{jk}) \\ &\quad \forall k, j, m, n \in \mathcal{R}_{jk}. \end{aligned} \quad (42)$$

By considering (38) and (42) for satisfying the inequality (29), it is sufficient that the following functional be positive for some M :

$$\mathcal{T}(\mathcal{B}_{jk}) \triangleq \varphi_{jk} - (1 - \mathcal{B}_{jk})\psi_{jk} \quad \forall j, k. \quad (43)$$

By considering $M = 2$ we can write

$$\varphi_{jk} = -\frac{L(L-1)(L-2)}{2} \mathcal{B}_{jk}^2 (1 - \mathcal{B}_{jk})^{L-3} \quad \forall j, k, \quad (44)$$

$$\begin{aligned} (1 - \mathcal{B}_{jk})\psi_{jk} &= L(L-1)(L-2)\mathcal{B}_{jk} \\ &\cdot \left(\frac{L-1}{2} \mathcal{B}_{jk} - 1 \right) (1 - \mathcal{B}_{jk})^{L-3} \quad \forall j, k. \end{aligned} \quad (45)$$

Thus, based on assumption (28) we can write

$$\begin{aligned} \mathcal{T}(\mathcal{B}_{jk}) &= -L(L-1)(L-2)\mathcal{B}_{jk} \left(\frac{L}{2} \mathcal{B}_{jk} - 1 \right) \\ &\cdot (1 - \mathcal{B}_{jk})^{L-3} > 0. \end{aligned} \quad (46)$$

Hence, it can be concluded that

$$\Phi_{jk}^{mn} > 0 \quad \forall k, j, m, n \in \mathcal{R}_{jk}. \quad (47)$$

(b) Consider the case $m = n$.

First, from assumption (28) and (44)-(45) it can be easily concluded that

$$\varphi_{jk}, \psi_{jk} < 0 \quad \forall j, k. \quad (48)$$

As usually we have $L \gg 1$; from (28) it can be concluded that $\mathcal{B}_{jk} \ll 1$. From (12) it can be easily concluded that $b_{ijk} \leq \mathcal{B}_{jk} \ll 1$, for all k, j, i , and based on (7) we have

$$b_{ijk} \ll 1 \implies \frac{\eta_{ijk}}{\sqrt{r_{ijk}}} > \sqrt{\frac{3}{2}}, \quad \begin{array}{l} 1 \leq j \leq n_k, \\ 1 \leq k \leq \mathcal{N}. \end{array} \quad (49)$$

From (36), (40), (44)-(45), and (49) it can be concluded that

$$\Phi_{jk}^i > 0 \quad \forall k, j, i \in \mathcal{R}_{jk}. \quad (50)$$

From (47) and (50) it can be deduced that, under assumption (28) and for $M = 2$, the theorem objective in relation (29) is satisfied. \square

Now, we propose another theorem based on which the existence and uniqueness of the solution vector of the system (23)–(25) that can be proved.

Theorem 2. *Assume that there exists one and only one congested link i for each path j of the video source k , for all j, k . Then, based on the assumption (28) in Theorem 1 and the following assumption, there exists a unique and optimal solution vector for the optimization problem (23)–(25):*

$$x_{jk} < e_{ijk} - \frac{2}{\Delta_{jk}} \quad \forall j, k, i. \quad (51)$$

Proof. First it must be shown that the Lagrangian (27) has positive second derivatives with respect to all of the x_{jk} variables. From (27) we can write the following:

$$\frac{\partial \Psi}{\partial x_{jk}} = \frac{\partial \mathcal{D}_T}{\partial x_{jk}} - \lambda_k - \lambda_{jk} \quad \forall j, k. \quad (52)$$

Also we have

$$\frac{\partial^2 \Psi}{\partial x_{jk}^2} = \frac{\partial^2 \mathcal{D}_T}{\partial x_{jk}^2} \quad \forall j, k. \quad (53)$$

From the definition of \mathcal{D}_T in (21), we can write

$$\frac{\partial^2 \mathcal{D}_T}{\partial x_{jk}^2} = \frac{2\theta_k}{(\mathcal{R}_k + \mathcal{R}_{k0})^3} + \sum_{k=1}^{\mathcal{N}} \xi_k \cdot \frac{\partial^2 p_T^k}{\partial x_{jk}^2} \quad \forall j, k. \quad (54)$$

Based on the definition of p_T^k in (20), we can write

$$\begin{aligned} \frac{\partial^2 \mathcal{D}_T}{\partial x_{jk}^2} &= \frac{2\theta_k}{(\mathcal{R}_k + \mathcal{R}_{k0})^3} + \xi_k \frac{\partial^2 p_{jk}}{\partial x_{jk}^2} \left[\prod_{\substack{u=1 \\ u \neq j}}^{n_k} (1 - p_{uk}) \right] \\ &+ \sum_{\substack{v=1 \\ v \neq k}}^{\mathcal{N}} \xi_v \frac{\partial^2 p_{uv}}{\partial x_{jk}^2} \left[\prod_{\substack{n=1 \\ n \neq u}}^{n_v} (1 - p_{nv}) \right] \quad \forall j, k. \end{aligned} \quad (55)$$

If we assume that the congestion-related and wireless-link losses are small enough, the equation (19) can be simplified as follows:

$$p_{jk} \approx p_{jk}^{\mathcal{R}} + p_{jk}^{\mathcal{Q}} \quad \forall j, k, \quad (56)$$

consequently

$$\frac{\partial p_{jk}}{\partial x_{jk}} = \frac{\partial p_{jk}^{\mathcal{R}}}{\partial x_{jk}} + \frac{\partial p_{jk}^{\mathcal{Q}}}{\partial x_{jk}} \quad \forall j, k. \quad (57)$$

We also have

$$\frac{\partial^2 p_{jk}}{\partial x_{jk}^2} = \frac{\partial^2 p_{jk}^{\mathcal{R}}}{\partial x_{jk}^2} + \frac{\partial^2 p_{jk}^{\mathcal{Q}}}{\partial x_{jk}^2} \quad \forall j, k. \quad (58)$$

From (10), we have

$$\frac{\partial r_{ijk}}{\partial x_{jk}} = 1 + \frac{\partial a_{ijk}}{\partial x_{jk}} \quad \forall j, k, i \in \mathcal{R}_{jk}. \quad (59)$$

In general, from congestion point of view, we can partition the wireless links in \mathcal{R}_{jk} to two other disjoint sets. One set is related to the congested links associated with common nodes in \mathcal{R}_{jk}^c which we denote by $\overline{\mathcal{R}}_{jk}$, and the other is associated with noncongested ones, that is, $\mathcal{R}_{jk} \setminus \overline{\mathcal{R}}_{jk}$. For congested links we can write simply

$$\frac{\partial a_{ijk}}{\partial x_{jk}} = -1 \implies \frac{\partial r_{ijk}}{\partial x_{jk}} = 0 \quad \forall j, k, i \in \overline{\mathcal{R}}_{jk}. \quad (60)$$

But, for noncongested links we have

$$\frac{\partial a_{ijk}}{\partial x_{jk}} = 0 \implies \frac{\partial r_{ijk}}{\partial x_{jk}} = 1 \quad \forall j, k, i \in \mathcal{R}_{jk} \setminus \overline{\mathcal{R}}_{jk}. \quad (61)$$

From chain rule, we can write

$$\frac{\partial p_{jk}^{\mathcal{R}}}{\partial x_{jk}} = \sum_{m=1}^{\mathcal{M}_{jk}-1} \frac{\partial p_{jk}^{\mathcal{R}}}{\partial r_{mjk}} \cdot \frac{\partial r_{mjk}}{\partial x_{jk}}. \quad (62)$$

And also

$$\begin{aligned} \frac{\partial^2 p_{jk}^{\mathcal{R}}}{\partial x_{jk}^2} &= \sum_{m=1}^{\mathcal{M}_{jk}-1} \sum_{n=1}^{\mathcal{M}_{jk}-1} \left(1 + \frac{\partial a_{mjk}}{\partial x_{jk}} \right) \\ &\cdot \left(1 + \frac{\partial a_{njk}}{\partial x_{jk}} \right) \frac{\partial^2 p_{jk}^{\mathcal{R}}}{\partial r_{mjk} \partial r_{njk}} \quad \forall j, k. \end{aligned} \quad (63)$$

From (60) and (61) we can write

$$\frac{\partial^2 p_{jk}^{\mathcal{R}}}{\partial x_{jk}^2} = \sum_{m \in \mathcal{R}_{jk} \setminus \overline{\mathcal{R}}_{jk}} \sum_{n \in \mathcal{R}_{jk} \setminus \overline{\mathcal{R}}_{jk}} \frac{\partial^2 p_{jk}^{\mathcal{R}}}{\partial r_{mjk} \partial r_{njk}} > 0. \quad (64)$$

From the definition of $p_{jk}^{\mathcal{Q}}$ in (14), it can be shown that

$$\frac{\partial^2 p_{jk}^{\mathcal{Q}}}{\partial x_{jk}^2} = \int_{\Delta_{jk}}^{\infty} \frac{\partial^2 \beta_{jk}(t)}{\partial x_{jk}^2} dt. \quad (65)$$

Now, we show that under assumption (51) and the fact that $\Delta_{jk} < 1$ we can write

$$\frac{\partial^2 \beta_{jk}(t)}{\partial x_{jk}^2} > 0. \quad (66)$$

From (18) we can rewrite the distribution $\beta_{jk}(t)$ as follows:

$$\begin{aligned} \beta_{jk}(t) &= \underbrace{\int_0^t \int_0^{\tau_{n-1}} \cdots \int_0^{\tau_2}}_{n-1} f_{njk}(t - \tau_{n-1}) \\ &\cdot f_{(n-1)jk}(\tau_{n-1} - \tau_{n-2}) f_{(n-2)jk}(\tau_{n-2} - \tau_{n-3}) \\ &\cdots f_{1jk}(\tau_1) d\tau_{n-1} \cdots d\tau_1 \quad \forall j, k, \end{aligned} \quad (67)$$

in which

$$n = \mathcal{M}_{jk} - 1. \quad (68)$$

But, based on the theorem assumption, as the congestion occurs only in one of the links in each path j of the source

k and the ingress node i associated with this congested link, works, and near the capacity region, from (16) and (17) we have

$$\alpha_{ijk} \rightarrow \infty. \quad (69)$$

Equivalently, we can say that the delay distribution function (67) of each path j of the source k can be approximated by the convolution of a dominant exponential delay distribution associated with this congested node and some other negligible delay distributions which behave like weighted dirac delta functions as compared with the dominant distribution as follows:

$$\beta_{jk}(t) \approx \frac{e^{-t/\alpha_{ijk}}}{\alpha_{ijk}} \quad \forall k, j. \quad (70)$$

Thus we have

$$\frac{\partial^2 \beta_{jk}(t)}{\partial x_{jk}^2} = \frac{\partial^2}{\partial x_{jk}^2} \left(\frac{e^{-t/\alpha_{ijk}}}{\alpha_{ijk}} \right) \quad \forall k, j. \quad (71)$$

Based on integral limits in (65), the theorem assumption (51), and the relation (70), we have

$$\frac{\partial^2 \beta_{jk}(t)}{\partial x_{jk}^2} = t \cdot \left(\frac{t}{\alpha_{ijk}} - 2 \right) e^{-t/\alpha_{ijk}} > 0 \quad \forall k, j, i \in \mathcal{R}_{jk}^c. \quad (72)$$

Based on (65) and (72), we can conclude that

$$\frac{\partial^2 p_{jk}^{\mathcal{Q}}}{\partial x_{jk}^2} > 0 \quad \forall j, k. \quad (73)$$

From (58), (64), and (73) we can conclude that

$$\frac{\partial^2 p_{jk}}{\partial x_{jk}^2} > 0 \quad \forall j, k. \quad (74)$$

Note that the first term of (55) is positive. Now, based on (74) it is easy to show that the second term of (55) is also positive. For proving the positiveness of the third term, we must show that

$$\frac{\partial^2 p_{uv}}{\partial x_{jk}^2} > 0 \quad \forall j, u, v \neq k, \quad (75)$$

or equivalently

$$\frac{\partial^2 p_{uv}^{\mathcal{R}}}{\partial x_{jk}^2} + \frac{\partial^2 p_{uv}^{\mathcal{Q}}}{\partial x_{jk}^2} > 0 \quad \forall j, u, v \neq k. \quad (76)$$

It is trivial that if path u of the source v is disjoint from path j of the source k , we have

$$\frac{\partial^2 p_{uv}}{\partial x_{jk}^2} = 0. \quad (77)$$

So, from now on, we assume that path u of the source v is common with path j of the source k in some links.

Similar to (32) we can write

$$\begin{aligned} \frac{\partial^2 p_{uv}^{\mathcal{R}}}{\partial r_{mjk} \partial r_{njk}} &= -\varphi_{uv} \frac{\partial^2 \mathcal{B}_{uv}}{\partial r_{mjk} \partial r_{njk}} - \psi_{uv} \frac{\partial \mathcal{B}_{uv}}{\partial r_{mjk}} \\ &\quad \cdot \frac{\partial \mathcal{B}_{uv}}{\partial r_{njk}} \quad \forall u, v, k, j, m, n \in \mathcal{R}_{uv}, \end{aligned} \quad (78)$$

where φ_{uv} and ψ_{uv} are defined as in (31) and (33), respectively.

Note that if $m \in \mathcal{R}_{uv}^c \cap \mathcal{R}_{jk}^c$, we have $r_{mjk} = r_{muv}$ and we can write

$$\begin{aligned} \frac{\partial \mathcal{B}_{uv}}{\partial r_{mjk}} &= \frac{\partial \mathcal{B}_{uv}}{\partial r_{muv}} = \left[\prod_{\substack{n=1 \\ n \neq m}}^{\mathcal{M}_{uv}} (1 - b_{n uv}) \right] \\ &\quad \cdot \frac{\eta_{muv} \cdot e^{-\eta_{muv}/r_{muv}}}{2\sqrt{2\pi}} r_{muv}^{-3/2} \quad \forall v, u, m \in \mathcal{R}_{uv}^c \cap \mathcal{R}_{jk}^c. \end{aligned} \quad (79)$$

On the other hand, if $m \notin \mathcal{R}_{uv}^c \cap \mathcal{R}_{jk}^c$, we have

$$\frac{\partial \mathcal{B}_{uv}}{\partial r_{mjk}} = 0. \quad (80)$$

Similarly, if $m, n \in \mathcal{R}_{uv}^c \cap \mathcal{R}_{jk}^c$, we have $r_{mjk} = r_{muv}$, $r_{njk} = r_{nuv}$ and we can write

$$\begin{aligned} \frac{\partial^2 \mathcal{B}_{jk}}{\partial r_{mjk} \partial r_{njk}} &= \frac{\partial^2 \mathcal{B}_{jk}}{\partial r_{muv} \partial r_{nuv}} = - \left[\prod_{\substack{d=1 \\ d \neq m, n}}^{\mathcal{M}_{uv}} (1 - b_{d uv}) \right] \\ &\quad \cdot \frac{\eta_{muv} \cdot \eta_{nuv} \cdot e^{-\eta_{muv}/r_{muv}} \cdot e^{-\eta_{nuv}/r_{nuv}}}{8\pi} \\ &\quad \cdot r_{muv}^{-3/2} \cdot r_{nuv}^{-3/2} \quad \forall k, j, u, v, m, n \in \mathcal{R}_{uv}^c \cap \mathcal{R}_{jk}^c, \end{aligned} \quad (81)$$

and also

$$\begin{aligned} \frac{\partial^2 \mathcal{B}_{uv}}{\partial r_{njk}^2} &= \frac{\partial^2 \mathcal{B}_{uv}}{\partial r_{nuv}^2} = \left[\prod_{\substack{m=1 \\ m \neq n}}^{\mathcal{M}_{uv}} (1 - b_{m uv}) \right] \\ &\quad \cdot \frac{\eta_{nuv} \cdot r_{nuv}^{-7/2} \cdot e^{-\eta_{nuv}/r_{nuv}}}{2\sqrt{2\pi}} \\ &\quad \cdot \left(\eta_{nuv}^2 - \frac{3}{2} r_{nuv} \right) \quad \forall u, v, k, j, n \in \mathcal{R}_{uv}^c \cap \mathcal{R}_{jk}^c. \end{aligned} \quad (82)$$

If m or $n \notin \mathcal{R}_{uv}^c \cap \mathcal{R}_{jk}^c$, we have

$$\frac{\partial^2 \mathcal{B}_{jk}}{\partial r_{mjk} \partial r_{njk}} = 0. \quad (83)$$

If $n \notin \mathcal{R}_{uv}^c \cap \mathcal{R}_{jk}^c$, we have

$$\frac{\partial^2 \mathcal{B}_{uv}}{\partial r_{njk}^2} = 0. \quad (84)$$

Similar to the results in Theorem 1 for $M = 2$, we have

$$\frac{\partial^2 p_{uv}^{\mathcal{R}}}{\partial r_{mjk} \partial r_{njk}} > 0 \quad \forall u, v, k, j, m, n \in \mathcal{R}_{uv}^c \cap \mathcal{R}_{jk}^c. \quad (85)$$

And if m or $n \notin \mathcal{R}_{uv}^c \cap \mathcal{R}_{jk}^c$, we have

$$\frac{\partial^2 p_{uv}^{\mathcal{R}}}{\partial r_{mjk} \partial r_{njk}} = 0. \quad (86)$$

Similar to (63) we can write

$$\begin{aligned} \frac{\partial^2 p_{uv}^{\mathcal{R}}}{\partial x_{jk}^2} &= \sum_{m=1}^{\mathcal{M}_{uv}-1} \sum_{n=1}^{\mathcal{M}_{uv}-1} \left(1 + \frac{\partial a_{muv}}{\partial x_{jk}} \right) \\ &\cdot \left(1 + \frac{\partial a_{nuv}}{\partial x_{jk}} \right) \frac{\partial^2 p_{uv}^{\mathcal{R}}}{\partial r_{muv} \partial r_{nuv}} \quad \forall j, k, u, v. \end{aligned} \quad (87)$$

If we define $\mathcal{W}_{uvjk} \triangleq \mathcal{R}_{jk}^c \cap \mathcal{R}_{uv}^c \setminus \overline{\mathcal{R}}_{uv}$, then

$$\frac{\partial^2 p_{uv}^{\mathcal{R}}}{\partial x_{jk}^2} = \sum_{m \in \mathcal{W}_{uvjk}} \sum_{n \in \mathcal{W}_{uvjk}} \frac{\partial^2 p_{uv}^{\mathcal{R}}}{\partial r_{muv} \partial r_{nuv}} \geq 0. \quad (88)$$

Thus, from (85)–(88) we have

$$\frac{\partial^2 p_{uv}^{\mathcal{R}}}{\partial x_{jk}^2} \geq 0 \quad \forall j, k, u, v. \quad (89)$$

Similar to the steps in (65)–(73) we can write

$$\frac{\partial^2 p_{uv}^{\mathcal{Q}}}{\partial x_{jk}^2} \geq 0 \quad \forall j, k, u, v. \quad (90)$$

Thus we can write

$$\frac{\partial^2 p_{uv}}{\partial x_{jk}^2} \geq 0 \quad \forall j, k, u, v. \quad (91)$$

Now, from (91) we can conclude that the third term in (55) must be positive, and finally based on (55), (74), and (91), we have

$$\frac{\partial^2 \mathcal{D}_T}{\partial x_{jk}^2} > 0 \quad \forall j, k. \quad (92)$$

From (92) and the convexity of the constraint set (24)–(25) and (51), it can be deduced that the constrained optimization problem (23) has a unique and optimal solution vector χ^* [16]. \square

Theorem 3. Assume $\mathcal{M}_{jk}-1 > 1$ and consider the general form of Theorem 2 in which there exists the possibility of multiple congested links in path j of the video source k . Based on the assumption (28) in Theorem 1 and the following assumption, there exists a unique and optimal solution vector for the optimization problem (23)–(25):

$$\Delta_{jk} > \frac{-\partial \sigma_{jk} / \partial x_{jk} + \sqrt{(\partial \sigma_{jk} / \partial x_{jk})^2 - \sigma_{jk} (\partial^2 \sigma_{jk} / \partial x_{jk}^2)}}{\sigma_{jk}} \quad \forall j, k, \quad (93)$$

in which

$$\sigma_{jk} \triangleq \prod_{i=1}^{\mathcal{M}_{jk}-1} (\alpha_{ijk})^{-1}. \quad (94)$$

Proof. It is clear that the delay distribution function of each node has exponential form. Equation (67) can be rewritten for $n = \mathcal{M}_{jk} - 1 > 2$ as follows:

$$\begin{aligned} \beta_{jk}(t) &= \underbrace{\int_0^t \int_0^{t-\tau_{n-1}} \cdots \int_0^{t-\sum_{m=2}^{n-1} \tau_m}}_{n-1} \prod_{m=1}^n f_{mjk}(\tau_{m-1}) \\ &\cdot f_{2jk} \left(t - \sum_{m=1}^{n-1} \tau_m \right) d\tau_{n-1} \cdots d\tau_1 \quad \forall j, k. \end{aligned} \quad (95)$$

For $n = 2$ we have

$$\beta_{jk}(t) = \int_0^t f_{1jk}(\tau_1) f_{2jk}(t - \tau_1) d\tau_1 \quad \forall j, k. \quad (96)$$

From preliminary calculus and the definition of $f_{ijk}(\cdot)$ in (15), the equation (95) can be simplified as follows:

$$\beta_{jk}(t) = \prod_{i=1}^{\mathcal{M}_{jk}-1} s_{ijk} e^{-s_{ijk} t} \cdot \mathcal{A}_{jk}(t) \quad \forall j, k, \quad (97)$$

in which

$$s_{ijk} \triangleq \alpha_{ijk}^{-1} \quad \forall j, k, i, \quad (98)$$

and for $n = \mathcal{M}_{jk} - 1 > 2$ we have

$$\mathcal{A}_{jk}(t) \triangleq \underbrace{\int_0^t \int_0^{t-\tau_{n-1}} \cdots \int_0^{t-\sum_{m=2}^{n-1} \tau_m}}_{n-1} e^{-u_{jk}(t)} d\tau_{n-1} \cdots d\tau_1 \quad \forall j, k, \quad (99)$$

in which

$$\begin{aligned} u_{jk}(t) &\triangleq \sum_{m=3}^n (s_{mjk} - s_{1jk}) \tau_{m-1} + (s_{2jk} - s_{1jk}) \\ &\cdot \left(t - \sum_{m=1}^{n-1} \tau_m \right) \quad \forall j, k, \end{aligned} \quad (100)$$

for $n = 2$ we have

$$\mathcal{A}_{jk}(t) \triangleq \int_0^t e^{-u_{jk}(t)} d\tau_1 \quad \forall j, k, \quad (101)$$

in which

$$u_{jk}(t) \triangleq (s_{2jk} - s_{1jk})(t - \tau_1). \quad (102)$$

It can be deduced from (15) and (100) that $\mathcal{A}_{jk}(\cdot) > 0$ is not a function of x_{jk} . So, in order for (65) to be positive and based on (97), it is sufficient that we have

$$\frac{\partial^2}{\partial x_{jk}^2} \prod_{i=1}^{\mathcal{M}_{jk}-1} s_{ijk} e^{-s_{ijk} t} = \frac{\partial^2}{\partial x_{jk}^2} \sigma_{jk} e^{-s_{ijk} t} > 0 \quad \forall j, k. \quad (103)$$

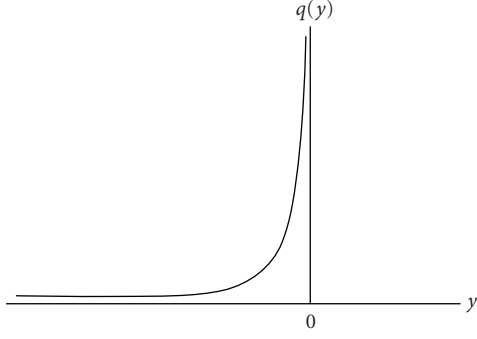


FIGURE 3: Typical penalty function.

By taking derivatives and considering the fact that $t \geq \Delta_{jk}$, for proving the positiveness of (103), it is sufficient that

$$\frac{\partial^2 \sigma_{jk}}{\partial x_{jk}^2} + 2t \frac{\partial \sigma_{jk}}{\partial x_{jk}} + t^2 \sigma_{jk} > 0 \quad \forall j, k. \quad (104)$$

Since $\sigma_{jk} \geq 0$, it is sufficient that

$$t > \frac{-\partial \sigma_{jk} / \partial x_{jk} + \sqrt{(\partial \sigma_{jk} / \partial x_{jk})^2 - \sigma_{jk} (\partial^2 \sigma_{jk} / \partial x_{jk}^2)}}{\sigma_{jk}} \quad \forall j, k, \quad (105)$$

which is valid when assumption (93) is true and also $t \geq \Delta_{jk}$. The rest of the proof is the same as that of Theorem 2. \square

3.2. Corollary A. In the special case of equal delay distribution function for all of the nodes in path j of the source k , it can be easily shown that the assumption (93) can be simplified as follows:

$$x_{jk} < e_{jk} - \frac{\mathcal{M}_{jk} - 1 + \sqrt{\mathcal{M}_{jk} - 1}}{\Delta_{jk}} \quad \forall j, k. \quad (106)$$

It can be verified that the assumption (51) is a special case of the condition (106) for $\mathcal{M}_{jk} = 2$.

3.3. Corollary B. It can also be easily verified that, in the special case of equal delay distribution function for all of the nodes in path j of the source k , the distribution (97) reduces to the well-known *gamma* form [23] as follows:

$$\beta_{jk}(t) = \Gamma_t(\mathcal{M}_{jk} - 1; \alpha_{jk}) \triangleq \frac{t^{\mathcal{M}_{jk} - 2} e^{-t/\alpha_{jk}}}{(\mathcal{M}_{jk} - 2)! \alpha_{jk}^{\mathcal{M}_{jk} - 1}}. \quad (107)$$

Many iterative methods have been proposed which lead to the optimal solution of constrained optimization problem (23)–(25) with the additional assumptions in (28) and (51) or (93) [16]. From these methods we have selected the penalty function approach. A typical convex penalty function is depicted in Figure 3.

For solving the previous constrained optimization problem, it is adequate to solve the following unconstrained one [16]:

$$\mathcal{V}(\chi) \triangleq \mathcal{D}_T + \sum_k \int_0^{x_k^{\min} - \sum_j x_{jk}} q(y) dy. \quad (108)$$

Theorem 4. Assume that (28) and (51) or (93) are true and consider the following update rule:

$$\frac{d}{dt} x_{jk} = -\delta_{jk} \frac{\partial}{\partial x_{jk}} \mathcal{V}(\chi) \quad \forall j, k, \quad (109)$$

where $\delta_{jk} > 0$ is a small positive constant. Then, the function $\mathcal{V}(\cdot)$ is a Lyapunov function for the mentioned system (109) to which all the trajectories converge.

Proof. First, we must show that $\mathcal{V}(\cdot)$ is convex. From (92) and the convexity of function $q(\cdot)$, we have

$$\frac{\partial^2 \mathcal{V}}{\partial x_{jk}^2} = \frac{\partial^2 \mathcal{D}_T}{\partial x_{jk}^2} + q' \left(x_k^{\min} - \sum_j x_{jk} \right) > 0 \quad \forall j, k. \quad (110)$$

From (108)–(109) and the chain-rule, we can write

$$\begin{aligned} \dot{\mathcal{V}}(\chi) &\triangleq \frac{d\mathcal{V}}{dt} = \sum_k \sum_j \frac{\partial \mathcal{V}}{\partial x_{jk}} \cdot \frac{dx_{jk}}{dt} \\ &= -\sum_k \sum_j \delta_{jk} \left(\frac{\partial \mathcal{V}}{\partial x_{jk}} \right)^2 \leq 0. \end{aligned} \quad (111)$$

Thus, $\mathcal{V}(\cdot)$ is a Lyapunov function for the continuous-time system (109), and the vector χ^* is an equilibrium point of the system (23)–(25) to which all of the trajectories converge. \square

As we can see from assumptions (28) and (51), for guaranteeing the uniqueness of the solution vector in optimization problem (23)–(25), it is necessary that the x_{jk} variables remain in the constraint set ζ . So, we must solve a projected version of unconstrained optimization (108) [16]. The iterative gradient descent solution for solving the unconstrained problem (108) is as follows:

$$x_{jk}[n+1] = \left\{ x_{jk}[n] - \delta_{jk} \frac{\partial \mathcal{V}}{\partial x_{jk}} \Big|_{x_{jk}=x_{jk}[n]} \right\}_{x_{jk}[n] \in \zeta} \quad \forall j, k, \quad (112)$$

where δ_{jk} is some positive and sufficiently small constant that guarantees the convergence [15].

The stability of the discrete-time iteration (112) can be proved in the same way as that proposed in [15].

3.4. Note. In reality, due to the nodes mobility, there may exist estimation errors or uncertainties in some of the parameters (e.g., link capacities) associated with constrained optimization problem (23)–(25). This may cause an optimal and unique solution that can hardly be derived or cannot be

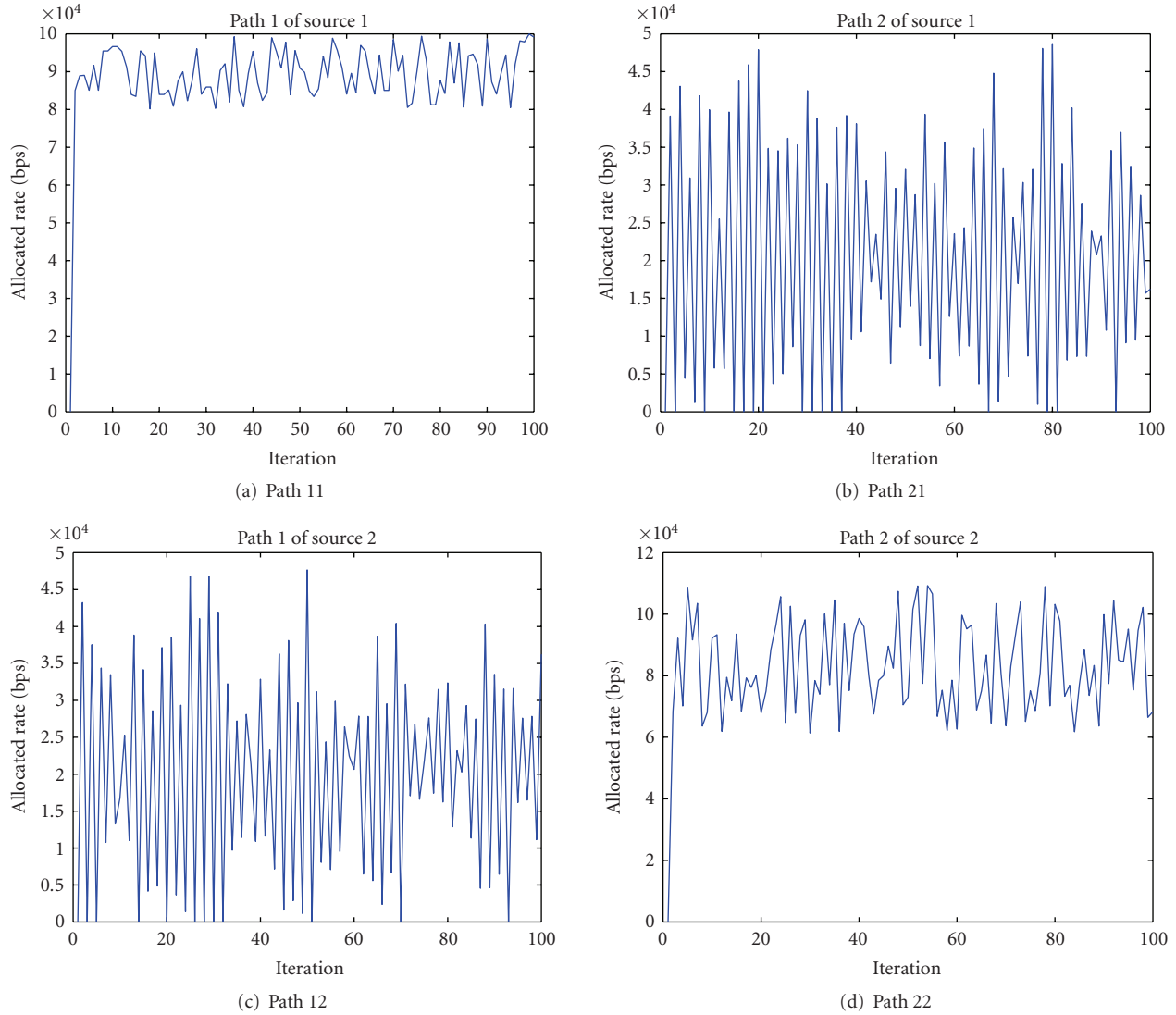


FIGURE 4: Rate allocation to different paths of the two sources.

reached at all by the proposed iterative algorithm in (112). Hence, some modifications must be applied in the proposed method. In general, if it can be assumed that the estimation error in the link capacities is such that the resulting uncertain constraint set ζ in (112) can be a subset of a given uncertainty set \mathcal{U} , then it can be shown that by adopting the *robust convex optimization* theory [24, 25], an optimal solution can still be found.

4. Numerical Analysis

Consider a sample scenario which is depicted in Figure 2. This scenario is consisted of two competing video sources S1 and S2, and each video source is routed through two disjoint paths. Path 2 of the source 1 and path 1 of the source 2 are common in one wireless link. 16 nodes are randomly distributed in a 10 m × 10 m area in this scenario. We have selected a simplified LOS propagation model for

mobile nodes, and the nodes mobility has been neglected by the assumption of a static network topology. Some typical η_{ij} and \mathcal{C}_{ijk} parameters are listed in Tables 1 and 2, respectively, (note that, e.g., Path 21 in Table 2 denotes path 2 of the source 1). Although these parameters are chosen arbitrarily and may not be necessarily practical one selection of other values cannot change the optimality of the results because the proposed optimization framework leads to optimal resource allocation with minimal total distortion to the competing video sources independent of the selection of η_{ij} and \mathcal{C}_{ijk} parameters. $M = 2$, $\mathcal{N} = 2$, $L = 1000$, and $x_{1,\min} = x_{2,\min}$ are selected to be 128 Kbps. Path 1 of the source 1 and path 2 of the source 2’s cross traffics are selected to be CBR sources with rates 20 Kbps and 50 Kbps, respectively, and other links’ cross traffics are being neglected. We assume that the paths 1 and 2 of source 1 are consisted of 4 and 5 wireless links, respectively. Also assume that the paths 1 and 2 of source 2 are consisted of 5 and 4 wireless links, respectively. Δ_{jk} parameter is assumed to be 5 milliseconds for each j, k

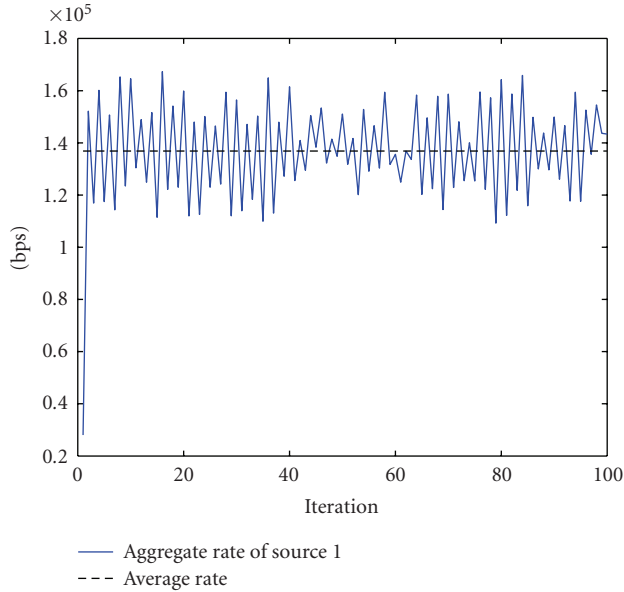


FIGURE 5: Aggregate rate of source 1.

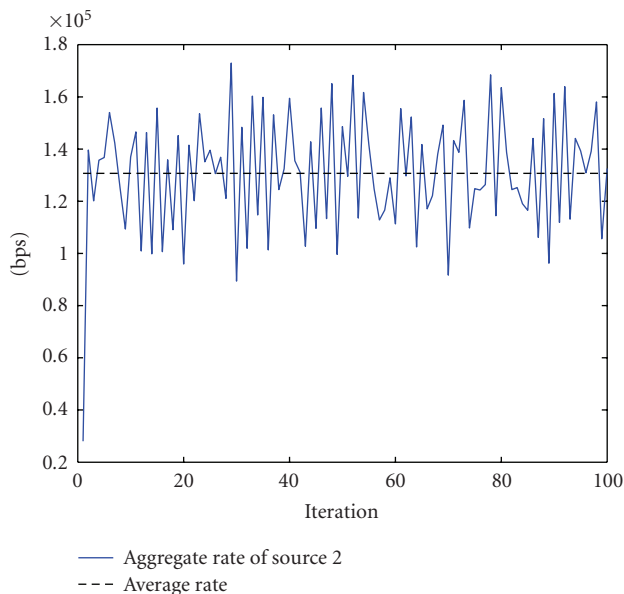


FIGURE 6: Aggregate rate of source 2.

TABLE 1: Values of the parameters η_{ij} .

η_{ij}	Link 1	Link 2	Link 3	Link 4	Link 5
Path 1	1	2	1.5	3	
Path 2	1	1	2	3	1.7
Path 3	4	2	1	1	2.1
Path 4	1.2	1.3	2	3.1	

because this value is typical for most practical video delivery applications. δ_{jk} in iteration (112) is assumed to be 0.07.

The allocated rate to each path of the two video sources is shown in the Figure 4, and the aggregate-allocated rate

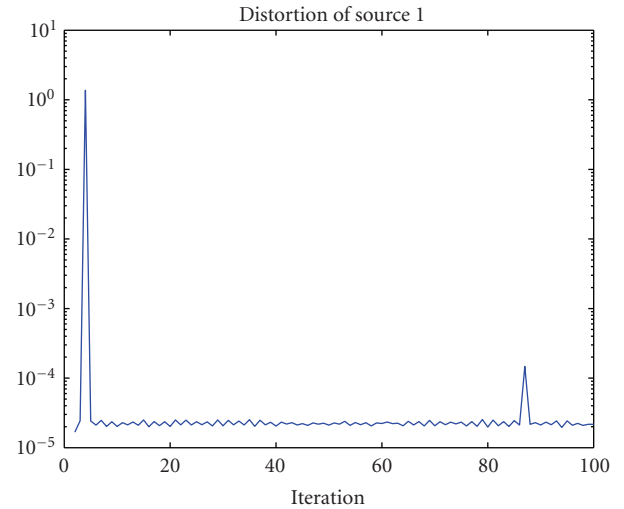


FIGURE 7: Distortion of source 1.

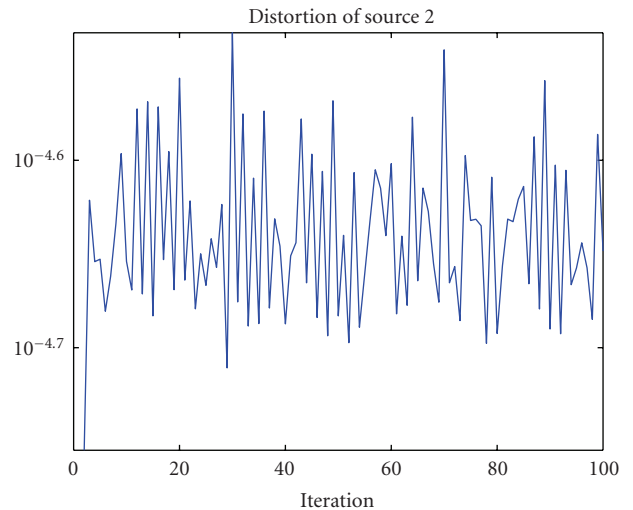


FIGURE 8: Distortion of source 2.

TABLE 2: Values of the link capacities (Kbps).

C_{ijk}	Link 1	Link 2	Link 3	Link 4	Link 5
Path 11	120	110	120	120	
Path 21	60	60	50	60	60
Path 12	70	70	50	70	70
Path 22	110	110	100	110	

to source-destination pairs is depicted in Figures 5 and 6. Note that, in Figures 5 and 6, the average aggregate rate of video sources 1 and 2 is above the threshold $x_{\min} = 128$ Kbps (1283 Kbps and 129 Kbps, resp.). As it can be deduced from Figures 5 and 6, the aggregate-allocated rate to the video sources makes some fluctuations around the target rate $x_{\min} = 128$ Kbps. This is the direct consequence of the competition process between the two video sources and the background traffic for consuming the network resources in the bottleneck links (link C in Figure 2). This results

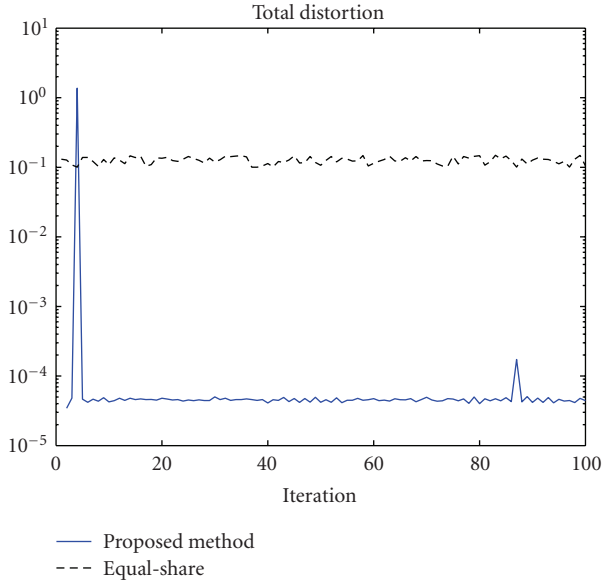


FIGURE 9: Total distortion comparison.

in fast fluctuation of the background traffic patterns for each video source. As the result of these fluctuations, the constraint set ζ in the problem (112) changes rapidly, and the iterative rate allocation algorithm (112) is not able to track the resulting fast variations in the constraint set; so it cannot converge to the optimal solution. One possible approach for faster convergence is the intelligent selection of the parameter δ_{jk} in (112) (e.g., incorporating the fuzzy logic [26] or genetic algorithm [27] in the selection process) based on the capacity estimation methods such as those in [28, 29].

In Figures 7 and 8, the distortion of the two sources ($\mathcal{D}_1, \mathcal{D}_2$) is being depicted, and as the source 1 suffers from more packet loss, its distortion performance is worse than that of source 2. Finally in Figure 9 the total distortion (\mathcal{D}_T) of the proposed method is compared with an equal share scenario. In equal share scenario, equal rate allocation pattern exists for the two source, that is, path 1 of the source 1 and path 2 of the source 2 each achieves 103 Kbps, and path 2 of source 1 and path 1 of source 2 each achieves the remaining $128 \text{ Kbps} - 103 \text{ Kbps} = 25 \text{ Kbps}$. As it can be easily checked, the total distortion of the proposed method is much less than that of the nonoptimal equal-share regime because the philosophy behind the resource allocation process in the equal-share scenario is far apart from that of the proposed distortion-minimal algorithm.

5. Conclusions

In the current work, an optimization framework is introduced by which the rate allocation to each path of a multipath wireless ad hoc network can be performed in such a way that the total distortion of multiple video sources resulting from the network congestion and wireless environment can be minimized.

Main application of such algorithms is in rate allocation to those subsets of real-time traffics which require a minimum level of total distortion. As we have used a simple LOS propagation model for the mobile nodes and ignored the mobility, a more powerful algorithm which can support more general multipath fading propagation models and the mobility can be considered for future research.

Acknowledgment

This work was supported by Iran Telecommunication Research Center (ITRC).

References

- [1] O. K. Tonguz and G. Ferrari, *Ad Hoc Wireless Networks: A Communication-Theoretic Perspective*, John Wiley & Sons, New York, NY, USA, 2006.
- [2] E. Royer and C.-K. Toh, "A review of current routing protocols for ad hoc mobile wireless networks," *IEEE on Personal Communications*, vol. 6, no. 2, pp. 46–55, 1999.
- [3] W. T. Webb and R. Steele, "Variable rate QAM for mobile radio," *IEEE Transactions on Communications*, vol. 43, no. 7, pp. 2223–2230, 1995.
- [4] T. Yoo and A. Goldsmith, "Throughput optimization using adaptive techniques," Tech. Rep., Wireless Systems Lab, Stanford University, Stanford, Calif, USA, 2004.
- [5] E. Setton and B. Girod, "Congestion-distortion optimized scheduling of video over a bottleneck link," in *Proceedings of the 6th IEEE Workshop on Multimedia Signal Processing (MMSP '04)*, pp. 179–182, Siena, Italy, September-October 2004.
- [6] E. Setton, X. Zhu, and B. Girod, "Congestion-optimized multi-path streaming of video over ad hoc wireless networks," in *Proceedings of IEEE International Conference on Multimedia and Expo (ICME '04)*, vol. 3, pp. 1619–1622, Taipei, Taiwan, June 2004.
- [7] R. Agarwal and A. Goldsmith, "Joint rate allocation and routing for multi-hop wireless networks with delay-constrained data," Tech. Rep., Wireless Systems Lab, Stanford University, Stanford, Calif, USA, 2004.
- [8] S. Adlakha, X. Zhu, B. Girod, and A. J. Goldsmith, "Joint capacity, flow and rate allocation for multiuser video streaming over wireless ad-hoc networks," in *Proceedings of the IEEE International Conference on Communications (ICC '07)*, pp. 1747–1753, Glasgow, Scotland, June 2007.
- [9] X. Zhu, S. Han, and B. Girod, "Congestion-aware rate allocation for multipath video streaming over ad hoc wireless networks," in *Proceedings of the International Conference on Image Processing (ICIP '04)*, vol. 4, pp. 2547–2550, Singapore, October 2004.
- [10] P. van Beek and M. U. Demircin, "Delay-constrained rate adaptation for robust video transmission over home networks," in *Proceedings of IEEE International Conference on Image Processing (ICIP '05)*, vol. 2, pp. 173–176, Genova, Italy, September 2005.
- [11] I. Haratcherev, J. Taal, K. Langendoen, R. Lagendijk, and H. Sips, "Optimized video streaming over 802.11 by cross-layer signaling," *IEEE Communications Magazine*, vol. 44, no. 1, pp. 115–121, 2006.
- [12] X. Zhu and B. Girod, "Media-aware multi-user rate allocation over wireless mesh network," in *Proceedings of the 1st Workshop*

- on Operator-Assisted (Wireless-Mesh) Community Networks (OpComm '06), pp. 1–8, Berlin, Germany, September 2006.
- [13] M. Handley, S. Floyd, J. Padhye, and J. Widmer, “TCP friendly rate control (TFRC): protocol specification,” Tech. Rep. RFC 3448, University of Mannheim, Mannheim, Germany, 2003.
- [14] X. Zhu and B. Girod, “Distributed rate allocation for multi-stream video transmission over ad hoc networks,” in *Proceedings of IEEE International Conference on Image Processing (ICIP '05)*, vol. 2, pp. 157–160, Genova, Italy, September 2005.
- [15] F. P. Kelly, A. K. Maulloo, and D. K. H. Tan, “Rate control for communication networks: shadow prices, proportional fairness and stability,” *Journal of the Operational Research Society*, vol. 49, no. 3, pp. 237–252, 1998.
- [16] D. P. Bertsekas and J. N. Tsitsiklis, *Parallel and Distributed Computation*, Prentice-Hall, Old Tappan, NJ, USA, 1989.
- [17] K. Stuhlmüller, N. Färber, M. Link, and B. Girod, “Analysis of video transmission over lossy channels,” *IEEE Journal on Selected Areas in Communications*, vol. 18, no. 6, pp. 1012–1032, 2000.
- [18] R. Chandramouli, K. P. Subbalakshmi, and N. Ranganathan, “Stochastic channel-adaptive rate control for wireless video transmission,” *Pattern Recognition Letters*, vol. 25, no. 7, pp. 793–806, 2004.
- [19] P. Feng, Z. Li, K. Lim, D. Wu, R. Yu, and G. Feng, “An adaptive rate control algorithm for video coding over personal digital assistants (pda),” in *Proceedings of the IEEE International Conference on Multimedia and Expo (ICME '03)*, vol. 2, pp. 573–576, Baltimore, Md, USA, July 2003.
- [20] R. Chandramouli, S. Kumar, and N. Ranganathan, “Joint optimization of quantization and on-line channel estimation for low bit-rate video transmission,” in *Proceedings of the IEEE International Conference on Image Processing (ICIP '98)*, vol. 1, pp. 649–653, Chicago, Ill, USA, October 1998.
- [21] K. Feher, *Wireless Digital Communication: Modulation and Spread Spectrum Applications*, Prentice-Hall, Old Tappan, NJ, USA, 1995.
- [22] A. Papoulis and S. U. Pillai, *Probability, Random Variables and Stochastic Processes*, McGraw-Hill, New York, NY, USA, 2002.
- [23] D. Bertsekas and R. Gallager, *Data Networks*, Prentice-Hall, Old Tappan, NJ, USA, 1987.
- [24] A. Ben-Tal and A. Nemirovski, “Robust convex optimization,” *Mathematics of Operations Research*, vol. 23, no. 4, pp. 769–805, 1998.
- [25] K. Zhou and J. C. Doyle, *Essentials of Robust Control*, Prentice-Hall, Old Tappan, NJ, USA, 1997.
- [26] P. Goudarzi and F. Sheikholeslam, “A fast fuzzy-based (Ω, α) -fair rate allocation algorithm,” in *Proceedings of the 19th IEEE International Parallel and Distributed Processing Symposium (IPDPS '05)*, p. 25b, Denver, Colo, USA, April 2005.
- [27] P. Goudarzi and R. Hassanzadeh, “A GA-based fuzzy rate allocation algorithm,” in *Proceedings of the IEEE International Conference on Communications (ICC '06)*, vol. 1, pp. 1–5, Istanbul, Turkey, June 2006.
- [28] L. Ning, G. Yan, and G. Li, “Fast capacity estimation algorithms for manets using directional antennas,” *Journal of Electronics*, vol. 24, no. 5, pp. 710–716, 2007.
- [29] J. Zhang, L. Cheng, and I. Marsic, “Models for non-intrusive estimation of wireless link bandwidth,” in *Proceedings of the 8th International Conference on Personal Wireless Communications (PWC '03)*, vol. 2775 of *Lecture Notes in Computer Science*, pp. 334–348, Venice, Italy, September 2003.